Exploring the random phase approximation: Application to CO adsorbed on Cu(111)

Xinguo Ren,[1,*] Patrick Rinke,[1,2] and Matthias Scheffler[1,2,3]
[1]*Fritz-Haber-Institut der Max-Planck-Gesellschaft, Faradayweg 4-6, D-14195 Berlin, Germany*
[2]*Materials Department, University of California, Santa Barbara, California 93106, USA*
[3]*Department of Chemistry and Biochemistry, University of California, Santa Barbara, California 93106, USA*
(Received 19 March 2009; revised manuscript received 7 June 2009; published 2 July 2009)

The adsorption of CO on the Cu(111) surface is investigated in the random phase approximation (RPA) as formulated within the adiabatic connection fluctuation-dissipation theorem. The RPA adsorption energy is obtained by adding a "local exchange-correlation correction" that is extrapolated from cluster calculations of increasing size, to the Perdew-Burke-Ernzerhof (PBE) value for the extended system. In comparison to density-functional theory calculations with the generalized gradient functionals PBE and AM05 and the hybrid functionals PBE0 and HSE03, we find a hierarchy of improved performance from AM05/PBE to PBE0/HSE03, and from PBE0/HSE03 to RPA, both in terms of the absolute adsorption energy as well as the adsorption-energy difference between the atop and the hollow fcc sites. In particular, the very weak atop site preference at the PBE0/HSE03 level is further stabilized by about 0.2 eV in the RPA. The mechanism behind this improvement is analyzed in terms of the *GW* density of states that gives a spectral representation en par with the RPA formalism for the total energy.

DOI: 10.1103/PhysRevB.80.045402 PACS number(s): 68.43.Bc, 71.15.Mb, 68.47.De

I. INTRODUCTION

Recent years have seen a revived interest in the chemisorption of carbon monoxide (CO) on metal surfaces. This is mainly due to the finding that density-functional theory (DFT), within its present-day local and semilocal approximations, fails to predict the correct adsorption site for CO on several transition- and noble-metal surfaces. In the low-coverage limit, different experiments consistently show that CO prefers the onefold-coordinated top site,[1–4] whereas both the local-density approximation (LDA) and several popular flavors (e.g., PW91, PBE, and RPBE) of the generalized gradient approximation (GGA) predict the threefold-coordinated hollow site to be the energetically most stable one.[5–7] Although cautionary remarks regarding convergence issues in today's DFT calculations have been raised,[8] it is nevertheless generally accepted that LDA and GGA fail for the (111) surface of Cu, Rh, and Pt, and this is often referred to as the "CO-adsorption puzzle."

The resurgence of the CO-adsorption puzzle is tied to the more fundamental quest of finding an "optimal" electronic-structure method that combines accuracy and tractability with transferability across different chemical environments. In this context the random phase approximation (RPA) is experiencing its own revived interest—facilitated in parts by the steady increase in available computer power—and a critical assessment of the RPA is beginning to emerge.[9–21] Since the CO-adsorption puzzle requires a good description for systems that are as diverse as metal surfaces and small molecules, it has become an important benchmark system for electronic-structure methods.[22–30] We will demonstrate in this paper that the RPA outperforms the common density functionals, because it combines exact exchange [as given by the Hartree-Fock (HF) expression] with a correlation energy based on the renormalized (screened) Coulomb potential that is finite for metallic systems and yields the right decay behavior outside a metal surface.[19] Further insight into the RPA's performance is gained from the excitation spectrum, computed with the associated *GW* self-energy.[31]

The most widely accepted explanation for the bonding mechanism of CO [and in fact many other molecules, e.g., H_2, O_2, and NO (Refs. 32 and 33)] to the metal surface is now based on the Blyholder model,[34] which describes the formation of the chemical bond between CO and the transition-metal surface by a donation–back-donation process. Due to their intrinsic deficiencies, LDA and GGA underestimate the position of the lowest unoccupied molecular orbital ($2\pi^*$) upon charge back-donation from the surface. This leads to an artificial enhancement of the binding interaction between the CO $2\pi^*$ orbital and the metal states, and thus an overestimation of the adsorption energy. For geometric reasons the error is more pronounced for the hollow site and in certain cases (Cu, Rh, and Pt) leads to the wrong energetic ordering.[6,22,23] A (semiempirical) energetic upward shift of the $2\pi^*$ level (e.g., by a Hubbard-*U*-type correction[22,24] or an extrapolation based on the configuration-interaction method[23]) makes a partial charge transfer from the metal surface to the $2\pi^*$ level more difficult and the correct adsorption site is recovered.

Supplementing semilocal exchange correlation (XC) with a fraction of exact exchange reduces the self-interaction error and increases the splitting between the 5σ and the $2\pi^*$ levels.[25–28] Among these so-called hybrid functionals—B3LYP,[35] PBE0,[36,37] and HSE03[38] are the most prominent types—PBE0 and HSE03 give the correct atop adsorption site for Cu and Rh but fail for Pt.[27] B3LYP does predict the correct adsorption for Pt,[25] but a more systematic investigation indicates that the success of B3LYP is rather fortuitous and comes at the expense of considerably worsening the properties of the metal substrate.[28] It appears that neither the current semilocal nor hybrid XC functionals can satisfactorily describe these metal-adsorbate systems as a whole and more sophisticated approaches are required. For finite clusters with a few tens of atoms, standard quantum

chemical methods [such as Møller-Plesset (MP) perturbation theory, the coupled cluster method, etc.] or quantum Monte Carlo have become tractable. Applying these methods in the framework of the "local XC correction" approach[29] considerably reduces the variation in the adsorption energies with cluster size and geometry in straightforward cluster calculations.

This indicates that accurate cluster calculations in the "local XC correction" scheme provide a viable approach to tackle the CO-adsorption puzzle and surface-adsorption problems in general. To exploit the usefulness of this approach it then becomes critical to choose appropriate quantum chemical or many-body methods for cluster calculations that are both accurate and computationally feasible. MP2 is the "cheapest" post-Hartree-Fock method and performs very well for small organic molecules.[39] However, it is known that MP2 diverges for three-dimensional metallic system and it is doubtful that MP2 calculations for considerably larger clusters (in the extended surface limit) will give physically meaningful results.[29] Very accurate quantum chemical methods such as CI or the coupled cluster method, on the other hand, tend to be extremely expensive, which limits their applicability.

Here we go beyond standard DFT by means of the RPA. In the RPA exchange is treated at the exact-exchange level [given by the HF expression for the exchange energy but evaluated with Kohn-Sham (KS) orbitals]. The "exact exchange" in RPA in general differs from both the HF exchange and exact exchange in the optimized effective potential sense (OEPx or also often referred to as EXX).[40,41] Although in all three cases the expression for the exchange energy is identical, the wave functions used to evaluate it differ.[41,42] In HF the wave functions are subjected to a nonlocal potential, whereas in OEPx the potential is local. The RPA wave functions, if computed self-consistently, will in turn differ from both the OEPx and HF ones. We will return to the issue of wave functions in RPA later.

The correlation energy in RPA is given by an infinite summation of the "ring diagrams." This infinite summation renormalizes or in other words *screens* the bare Coulomb interaction. The RPA originates from the treatment of the homogeneous electrons gas in many-body perturbation theory (MBPT), where a partial resummation of higher-order diagrams was found to be crucial to remove the divergence of the many-body expansion in terms of the bare Coulomb interaction.[43,44] Alternatively the RPA can be derived in the framework of density-functional theory via the adiabatic connection fluctuation-dissipation (ACFD) theorem,[45,46] in which the correlation energy is expressed in terms of the response function. From the ground-state DFT perspective, ACFD-RPA belongs to the fifth rung of Perdew's "Jacob's ladder" for XC functionals[47] and is currently the most widely applied approach to compute RPA total energies for realistic systems.

Several of the RPA's features have lead to the revived interest in recent years: first, in contrast to LDA and GGA, RPA incorporates exact exchange and is therefore self-interaction (although not self-polarization[48]) free. Second, in contrast to Møller-Plesset perturbation theory (e.g., MP2), the bare Coulomb interaction is renormalized (screened) in RPA, and the RPA correlation energy does not suffer from the divergence problem for metallic systems. Third, RPA yields the correct long-range behavior of the XC potential,[9] and thus the correct asymptotic power-law form of the dispersion interaction for various systems[10] as well as the right decay outside a metal surface.[19]

RPA calculations have been performed for atoms,[11,12,49] small molecules,[13,14] jellium slabs[15] and clusters,[16] layered systems,[17] noble-gas solids,[18] and molecular crystals.[21] Very recently, the RPA (with additional approximations) has also successfully been applied to a different adsorption problem [PTCDA on Ag(111)].[19] The general consensus that emerges from these studies is that, although the absolute RPA correlation energies are often overestimated (e.g., in the case of atoms[11,13,49] and the homogeneous electron gas[50]), the physically relevant energy differences, e.g., atomization energies,[13] are given rather accurately. For instance, the RPA correlation contribution to atomization energies is three times more accurate than the PBE one.[13,51,52] More importantly, the weak interaction in rare-gas solids and layered structures, which is beyond the reach of LDA, GGA, and hybrid functionals, is captured by the RPA.[17,18] Despite its apparent success, there are also shortcomings. Atomization energies of (small) molecules, for example, are not at chemical accuracy (± 43 meV) and a systematic underbinding is observed.[11,13,51] While it would be desirable to achieve higher accuracies by going beyond RPA, RPA itself constitutes an important next step, and it is crucial to establish its performance in different situations. In this context CO adsorption at metal surfaces provides an additional stringent benchmark system for future development beyond the RPA that incorporates features absent from previous benchmark systems.[22–30]

RPA calculations are most commonly performed as post-correction to a preceding standard DFT calculation. In analogy to OEPx and HF, a self-consistent solution of the RPA requires either a local (within the framework of ACFD) or a nonlocal (within MBPT) potential. The nonlocal potential in this case is given by the *GW* (Ref. 31) self-energy,[53–57] and the corresponding local potential[55–57] can be obtained through the Sham-Schlüter equation.[58–60] The calculation of the *GW* self-energy and, in particular, the solution of the Sham-Schlüter equation are computationally much more demanding tasks than calculating the RPA correlation energy with given orbitals, and hence a self-consistent solution of the RPA is rarely attempted. In this paper we exploit the relation between the RPA and the *GW* self-energy to calculate electronic excitation spectra that are consistent with the RPA. *GW* is currently the method of choice for calculating quasiparticle spectra in solids as measured by direct and inverse photoemission spectroscopy[42,61,62] and, as we will demonstrate below, also gives an excellent electron affinity and ionization potential for the free CO molecule.

The paper is organized as follows. In Sec. II the computational formalism is introduced. The results are presented in Sec. III; in Sec. III A for the free CO molecule and in Sec. III B for CO on Cu(111). An analysis based on the *GW* density of states (DOS) will be given in Sec. III C. Section IV concludes this paper.

II. COMPUTATIONAL APPROACH

Within ACFD, the RPA correlation energy is given by[45,46]

$$E_c^{\mathrm{RPA}} = \frac{1}{2\pi}\int_0^\infty du\ \mathrm{Tr}\{\ln[1-\chi_0(iu)v]+\chi_0(iu)v\}, \quad (1)$$

where $\mathrm{Tr}=\int d\mathbf{r}\int d\mathbf{r}'$, $v=1/|\mathbf{r}-\mathbf{r}'|$ is the bare Coulomb potential, and χ_0 is the dynamical-response function of the noninteracting KS system. The calculation of χ_0 involves both the occupied and unoccupied KS spin orbitals $\psi_{n\sigma}(\mathbf{r})$, their energies $\epsilon_{n\sigma}$, and their occupation factors $f_{n\sigma}$,

$$\chi_0(\mathbf{r},\mathbf{r}',iu) = \sum_\sigma \sum_{mn} \frac{(f_{m\sigma}-f_{n\sigma})}{iu+\epsilon_{n\sigma}-\epsilon_{m\sigma}} \times \psi^*_{m\sigma}(\mathbf{r})\psi_{n\sigma}(\mathbf{r})\psi^*_{n\sigma}(\mathbf{r}')\psi_{m\sigma}(\mathbf{r}'). \quad (2)$$

Together with the Hartree-Fock expression for the exchange energy,

$$E_x = -\frac{1}{2}\sum_\sigma \sum_{nm}^{\mathrm{occ}} \int\int d\mathbf{r}\, d\mathbf{r}' \frac{\psi^*_{n\sigma}(\mathbf{r})\psi_{m\sigma}(\mathbf{r})\psi^*_{m\sigma}(\mathbf{r}')\psi_{n\sigma}(\mathbf{r}')}{|\mathbf{r}-\mathbf{r}'|}, \quad (3)$$

the RPA total energy is given by

$$E_{\mathrm{tot}}^{\mathrm{RPA}}[\{\psi_n\}] = T_s + E_{\mathrm{ext}} + E_h + E_x[\{\psi_n\}] + E_c^{\mathrm{RPA}}[\{\psi_n\}], \quad (4)$$

where T_s, E_{ext}, and E_h are the kinetic, the external, and the Hartree energies of the Kohn-Sham system, respectively. To attain self-consistency in the Kohn-Sham system, a new set of KS orbitals would have to be computed from the Kohn-Sham equation pertaining to Eq. (4). Since self-consistency in the RPA is a computationally demanding task, as alluded to in the Introduction, it has so far only been performed for simple systems.[54,57,63] Instead the RPA is commonly computed non-self-consistently starting from a preceding DFT calculation. In this case the RPA total energy is then given by

$$E_{\mathrm{tot}}^{\mathrm{RPA}}[\{\psi_n\}] = E_{\mathrm{tot}}^{\mathrm{DFT}} - E_{\mathrm{xc}}^{\mathrm{DFT}} + E_x[\{\psi_n\}] + E_c^{\mathrm{RPA}}[\{\psi_n\}], \quad (5)$$

where the exchange-correlation energy of the chosen DFT functional is replaced with the exchange-correlation energy in RPA. We would like to emphasize that $E_x[\{\psi_n\}]$ in this case is not equivalent to the exchange energy in Hartree-Fock, because the wave functions used to evaluate the expression are DFT rather than HF wave functions. These differences are generally small but not negligible.[64] For a free CO molecule, for example, the exact-exchange energy computed from LDA orbitals differs from HF by ~0.5 eV. We will quantify the dependence on the DFT starting point in Sec. III by computing the RPA total energies starting from different functionals. We will demonstrate that the adsorption energies and adsorption-energy differences are rather insensitive to the chosen starting point (here LDA, PBE, and PBE0), in agreement with previous observations for molecules by Furche[13] and Fuchs and Gonze.[14]

The adsorption energies are calculated using the local XC correction scheme.[29] In this scheme the adsorption energy of the metal-adsorbate system is retrieved from a local correction to the PBE adsorption energy computed for the full system. The correction is given by the adsorption-energy *difference* for a cluster that contains the adsorbate and a part of the metal surface

$$\Delta E_{\mathrm{ads}}^{\mathrm{cluster}} = E_{\mathrm{ads}}^{\mathrm{cluster}}(\mathrm{XC\text{-}better}) - E_{\mathrm{ads}}^{\mathrm{cluster}}(\mathrm{PBE}). \quad (6)$$

For "XC-better" we explore here the GGA-type functional AM05, the two hybrid functionals PBE0 and HSE03, and the ACFD-RPA. The success of the local XC-correction method lies in the fast and testable convergence of the correction with respect to the cluster size[29] and the infinite cluster-size limit can be obtained from a systematic convergence of $\Delta E_{\mathrm{ads}}^{\mathrm{cluster}}$. In addition, a distinct advantage of RPA cluster calculations over calculations in a repeated slab geometry (as required for periodic boundary conditions) is the absence of spurious long-ranged polarization effects introduced by neighboring slabs and the slow k-point convergence resulting from the dielectric anisotropy.[65]

For molecular-adsorption problems, an analysis of the electronic structure often provides insights for understanding the underlying bonding mechanism between the molecule and the substrate. As briefly discussed in the Introduction, the self-energy consistent with the RPA is given by the G_0W_0 approximation[31]

$$\Sigma(\mathbf{r},\mathbf{r}';\omega) = -\frac{i}{2\pi}\int d\omega' \int d\mathbf{r}'' G_0(\mathbf{r},\mathbf{r}'';\omega-\omega') \times W_0(\mathbf{r}'',\mathbf{r}';\omega'). \quad (7)$$

Here G_0 is the Green's function and $W_0=v/(1-\chi_0 v)$ is the screened Coulomb potential of the noninteracting KS system. This procedure will hereafter be referred to as G_0W_0.

Hartree-Fock, hybrid functionals, ACFD-RPA, and G_0W_0 have recently been implemented into the computer code package FHI-aims.[66] In FHI-aims single-particle states are expanded in terms of numeric atom-centered orbitals (NAOs). This basis is not only compact but also inherently local. RPA atomization energies for a test set of small molecules are in excellent agreement with those reported in the literature.[13] Details of our implementation will be published elsewhere.[67]

The Cu-cluster geometries are constructed by cutting out three-layer-thick segments from bulk Cu with a lattice constant obtained using PBE. Larger clusters are achieved by an increase in the lateral direction. On-top- and fcc hollow-site adsorptions are simulated by adding the CO molecule to the upper and the lower sides of the clusters, respectively. Thus, surface relaxation effects to the cluster corrections, i.e., the energy difference $E_{\mathrm{ads}}^{\mathrm{cluster}}(\mathrm{XC\text{-}better})-E_{\mathrm{ads}}^{\mathrm{cluster}}(\mathrm{PBE})$, which we expect to be small for the system under consideration, are not included. However, for the PBE adsorption-energy calculation of the full surface-adsorbate system (which serves as the reference here), these relaxation effects are taken into account and lead to a lowering of the PBE adsorption energy by approximately 50 meV. Surface relaxation effects to the cluster corrections should be even smaller. The adsorbate system is modeled by repeated five-layer $c(2\times4)$ slabs separated by 15 Å vacuum, optimized in PBE with only the first two layers allowed to relax. The bond distances between the C and the O atoms and the C atom and the cluster obtained from this relaxation are used for the cluster calculations.

TABLE I. Atomization energy E_b (in eV), equilibrium bond length R_e (in Å), vibrational frequency (in cm^{-1}), and HOMO and LUMO energies (in eV) of the free CO molecule calculated by LDA, PBE, PBE0, and RPA/G_0W_0 based on each. ΔSCF refers to excitation energies calculated by total energy differences in different charge states.

	E_b	R_e	ν	E_{HOMO}	E_{LUMO}
LDA	12.97	1.127	2179	−9.12	−2.25
LDA ΔSCF				−14.10	1.56
PBE	11.67	1.135	2128	−9.04	−2.00
PBE ΔSCF				−13.87	1.74
PBE0	11.09	1.123	2235	−10.75	−0.75
RPA/G_0W_0@LDA	10.40	1.138	2117	−13.31	1.74
RPA/G_0W_0@PBE	10.45	1.137	2115	−13.17	1.84
RPA/G_0W_0@PBE0	10.60	1.130	2173	−13.76	2.02
EXP	11.11[a]	1.128[a]	2170[a]	−14.00[a]	1.8[b]

[a]Reference 68.
[b]Reference 69.

III. RESULTS AND DISCUSSIONS

A. Free CO

Before we turn to the adsorbate system, it is illuminating to consider the isolated CO molecule first. Here ACFD-RPA is used for calculating the equilibrium CO bond length, atomization energy, and vibrational frequency, and G_0W_0 for the molecular-energy levels of CO (shown in Table I). Since ACFD-RPA and G_0W_0 are performed as a one-step perturbation, the starting-point dependence is checked by using LDA, PBE, and PBE0 ground states. In agreement with previous studies we found the convergence of the RPA correlation energy with respect to basis size to be slow. To ensure the convergence of the atomization energy to within 50 meV, we use a standard FHI-aims NAO basis "tier 4."[66] The atomization energies in LDA, PBE, and PBE0 are already converged to below 10 meV using the "tier 2"[66] basis.

Inspection of Table I illustrates that LDA overestimates the atomization energy drastically. PBE improves over LDA but still overbinds by about 0.6 eV, whereas the PBE0 functional performs best in this case. The RPA is insensitive to the starting point to within 0.2 eV but underbinds roughly by the same amount as PBE overbinds. For the bond length and the vibrational frequency the situation is reversed on the DFT side. LDA gives the best result with only a slight overbinding of 0.001 Å, while PBE underbinds and PBE0 overbinds. Correspondingly, the vibrational frequency is only slightly overestimated by 9 cm^{-1} in LDA, while it is (underestimated) overestimated much more strongly in (PBE) PBE0. RPA based on PBE0 gives an excellent bond length and vibrational frequency, whereas RPA@PBE and RPA@LDA both underbind more strongly with a vibrational mode that is too soft.

The highest occupied molecular orbital (HOMO) and lowest unoccupied molecular orbital (LUMO) of CO are given by the 5σ and the $2\pi^*$ orbitals, respectively. Both LDA and PBE place the KS HOMO too high and the KS LUMO too low in energy. PBE0 brings the HOMO/LUMO levels approximately halfway between the LDA/GGA values and the experimental value, whereas a quantitative agreement with experiment is achieved only at the G_0W_0 level. A slight starting-point dependence of the G_0W_0 results is again noticeable, but the variation is much smaller than the corrections it provides. One may note that, within LDA and GGA, much better HOMO and LUMO energies can be obtained using the ΔSCF method, i.e., by computing the total energy difference between the neutral and the positively (negatively) charged molecule (see Table I). However, the relevant entities in the CO-adsorption puzzle are the KS levels of the DFT calculation and not the ΔSCF HOMO/LUMO positions. Upon adsorption the donation–back-donation process between CO and metal surfaces raises the KS LUMO of CO. Unlike in exact KS, where the LUMO level would change discontinuously, in LDA and GGA both the HOMO (which goes downward in energy) and the LUMO change continuously. The "effective" LUMO of adsorbed CO is thus underestimated, which gives rise to the overestimated binding energy.

For all three quantities the RPA results follow the same pattern: RPA at PBE0 gives the best agreement with experiment followed by RPA at PBE and RPA at LDA. The latter two are very similar in magnitude. On the DFT side this systematic trend is not observed and different functionals perform better for different quantities.

B. RPA adsorption energy of CO/Cu(111)

The ACFD-RPA adsorption energy in this work is obtained by adding the XC correction extrapolated from the cluster calculations to the PBE value for the extended system, as described in Sec. II. Apart from RPA, the cluster corrections are also performed for the GGA-type functional AM05, and hybrid functionals PBE0 and HSE03 for comparison. In Fig. 1 the adsorption-energy differences, as defined by Eq. (6), are shown as a function of cluster size for both the atop- and the hollow-fcc- adsorption geometries and for different approaches. It can be clearly seen that the adsorption-energy *differences* converges quite fast with re-

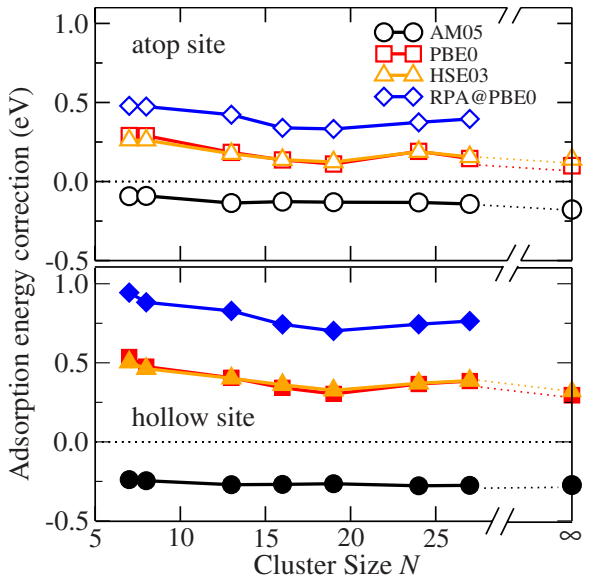

FIG. 1. (Color online) The adsorption-energy differences of four different functionals: AM05, PBE0, HSE03, and RPA@PBE0 with respect to PBE for the atop and the hollow fcc sites. The PBE0/HSE03 values in the periodic limit are from Ref. 27.

spect to cluster size, and the periodic limit can already be retrieved with good accuracy for clusters with approximately 20 Cu atoms. In Fig. 1 and in the following analysis the RPA results are based on PBE0 orbitals. Using LDA or PBE instead results in only small differences in the adsorption energy, as we will demonstrate later. Figure 1 illustrates that the correction to the PBE adsorption energies is positive for PBE0, HSE03, and RPA@PBE0 and will thus lead to a reduction in the adsorption energy. In AM05, however, the correction is negative leading to a further increase in the adsorption energies. For all four functionals, the magnitude of the correction at the hollow fcc site is approximately twice as large as that at the top site. For PBE0, HSE03 and RPA@PBE0 the reduction in adsorption energy is therefore accompanied by an increased tendency to favor the atop adsorption. For AM05, on the other hand, the increase in the adsorption energy leads to an even stronger preference of the incorrect hollow fcc site. The fact that AM05, which has been designed to give good surface energies,[70] produces even worse adsorption energies than PBE has also been observed and discussed by Stroppa and Kresse[28] for the example of CO on the Pt(111) surface. Stroppa *et al.* also noted that PBE0 and HSE03 give very similar adsorption energies[27] in agreement with our observation that the two lines are virtually indistinguishable in Fig. 1.

Figure 1 establishes the following hierarchy of decreasing adsorption energy: AM05, PBE, PBE0/HSE03, and RPA@PBE0. The correct adsorption-site preference is recovered already at the PBE0 (HSE03) level, but the PBE0 adsorption-energy difference for the two adsorption sites is almost vanishingly small (only a few tens of meV). The ACFD-RPA corrections to PBE0 are significant, with a further reduction of about 0.2 eV for the atop site and about 0.4 eV for the hollow site. This lifts the near degeneracy of the PBE0 results and gives a binding energy for the top site in much better agreement with experiment (see also Table II).

TABLE II. Adsorption energies of CO@Cu(111) for different approaches (units in eV). ΔE_{ads} is the adsorption-energy differences between the atop and the fcc sites and a negative value indicates the correct atop adsorption site.

	Top	fcc	ΔE_{ads}
E_{ads}(PBE)[a]	−0.71	−0.87	0.16
E_{ads}(PBE0)[a]	−0.61	−0.58	−0.03
E_{ads}(CASPT2)[b]	−0.49	>0	<−0.49
E_{ads}(EXP)	−0.46,[c] −0.49[d]		
This work			
E_{ads}(PBE)	−0.72	−0.86	0.14
E_{ads}(PBE0)	−0.58 ± 0.04	−0.54 ± 0.03	−0.04 ± 0.01
E_{ads}(RPA @ PBE0)	−0.37 ± 0.02	−0.15 ± 0.02	−0.22 ± 0.01

[a]Reference 27.
[b]Reference 30.
[c]Reference 3.
[d]Reference 71.

This is further exemplified in Fig. 2 where the difference of the corrections for the atop and the hollow sites is plotted for all four approaches. The dotted-dashed line marks the minimal correction that is needed to restore the correct adsorption-energy ordering. While PBE0 and HSE03 give only a slight on-top site preference, RPA stabilize this correct site preference further by about 0.2 eV. Conversely, the AM05 corrections go in the wrong direction.

In Table II we present our PBE, PBE0, and RPA@PBE0 adsorption energies for the infinite systems. They are obtained by adding the extrapolated cluster corrections to the PBE adsorption energy for the periodic slab calculation. The cluster corrections and the associated error bars are extracted from the last three points of the cluster calculations (Cu_{19}, Cu_{24}, and Cu_{27}; cf. Fig. 1). Previous theoretical calculations and available experimental results are also listed for comparison. The experimental adsorption energies[3,71] cited here were obtained indirectly from thermal-desorption-spectroscopy measurement by means of the Redhead model.[72]

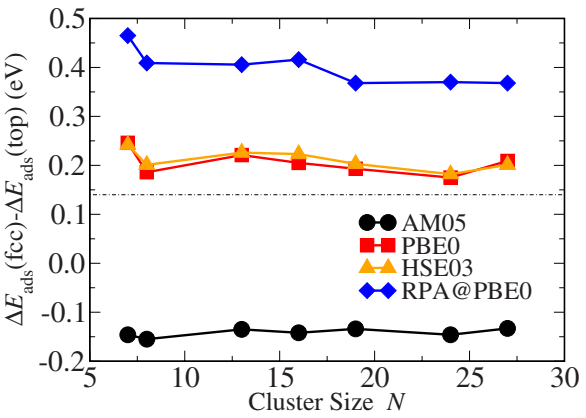

FIG. 2. (Color online) The site-preference energy corrections given by AM05, PBE0, HSE, and RPA@PBE0, with respect to PBE.

TABLE III. RPA adsorption energies (in eV) calculated for three different input ground states.

	RPA based on		
Site	LDA	PBE	PBE0
Top	-0.34 ± 0.01	-0.35 ± 0.01	-0.37 ± 0.02
fcc	-0.18 ± 0.01	-0.17 ± 0.01	-0.15 ± 0.02

Our PBE and PBE0 adsorption energies are in good agreement with previous plane-wave calculations,[27] which for the case of PBE0 confirms the validity of the local XC-correction approach. The RPA@PBE0 and PBE0 adsorption energies straddle the experimental values and the value obtained with multi-configuration second order perturbation theory (CASPT2) values and RPA underbinds by almost the same amount as PBE0 overbinds (~0.1 eV). The small underbinding in the RPA is similar to what was observed for free CO in Sec. III A and could be an intrinsic feature of the RPA. More important, however, are the adsorption-energy difference between the two (atop and hollow) sites since they provide evidence about the capability of an approach to capture subtle changes in the chemical environment and hence to produce reliable potential-energy surfaces. Here RPA@PBE0 and CASPT2 differ qualitatively; the latter does not bind CO at the fcc site.[30] while the former gives a binding energy of about −0.15 eV. Unfortunately for the fcc site the experimental situation is not as clear as for the atop site. There are, however indications from infrared-adsorption-spectroscopy measurements by Hayden *et al.*[73] and Raval *et al.*[4] that at temperatures below 100 K the threefold-coordinated site will eventually be populated as the CO coverage increases. The desorption temperature of approximately 90 K is indicative of an adsorption energy between 0.2 and 0.3 eV. This value is consistent with our RPA@PBE0 calculation for the low-coverage limit, if the influence of the lateral interactions between the CO molecules in the high-coverage limit is small.

Analogous to the free CO case, we have also investigated the sensitivity of the RPA adsorption energies on the starting point (i.e., the preceding ground-state calculation). Table III lists the extrapolated RPA@LDA, RPA@PBE, and RPA @PBE0 adsorption energies for the atop and the fcc hollow sites. The RPA adsorption energies prove to be very insensitive to the starting point, which is in agreement with observations made previously for small molecules.[14]

C. G_0W_0 density of states

To understand the mechanism behind the change in adsorption energy, it is illuminating to consider the electronic structure of the adsorbed system. Figures 3 and 4 compare the excitation spectrum of the free CO molecule with the DOS of CO adsorbed on a Cu_{16} cluster for the six approaches taken in this paper. As alluded to before, the G_0W_0 self-energy provides an electronic structure consistent with the RPA total-energy calculation from the many-body point of view. Panel (a) summarizes the molecular levels of free CO that were in parts presented in Sec. III A. PBE (and LDA) gives a HOMO level too high and a LUMO too low in energy. PBE0 improves over PBE and brings the HOMO and LUMO levels to approximately halfway between PBE and experiment whereas G_0W_0@PBE0 gives good agreement with experiment.

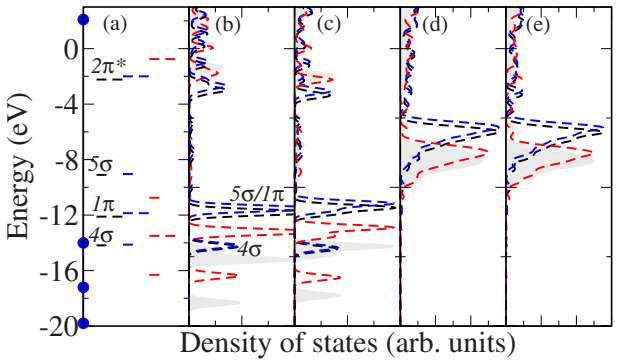

FIG. 3. (Color online) Orbital-energy levels of a free CO molecule and density of states from LDA (black dashed lines), PBE (blue dashed lines) and PBE0 (red dashed lines): orbital-energy levels [panel (a)]—experimental values are marked by blue circles—DOS projected on the CO orbitals of the CO/Cu_{16} cluster with CO adsorbed on the top site [panel (b)] and fcc hollow site [panel (c)] and DOS projected on the Cu orbitals on the top site [panel (d)] and hollow site [panel (e)]. The gray shaded region corresponds to the G_0W_0@PBE0 results shown in red in Fig. 4.

For CO adsorbed on Cu the molecular levels broaden into resonances due to hybridization with the metal states [panels (b) and (c)] but the trend observed for free CO carries over: the effective gap of adsorbed CO increases systematically from PBE to PBE0, and from PBE0 to G_0W_0@PBE0. In panels (d) and (e), the DOS projected on the Cu atoms is shown for the atop and the hollow sites, respectively. The pronounced peak originates mainly from the Cu *d* states. They are pushed toward higher binding energy when going from PBE to PBE0 but remain essentially unchanged from PBE0 to G_0W_0. It is important to emphasize that the evolution of the electronic DOS calculated with these three methods of increased sophistication matches the changes in the adsorption energies very well. In essence, the adsorption energy reduces as the effective CO HOMO-LUMO gap and the

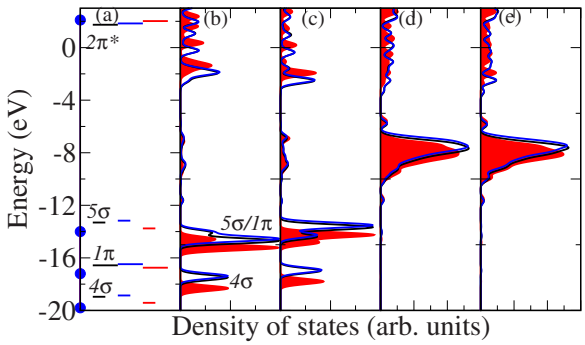

FIG. 4. (Color online) same as Fig. 3 but with G_0W_0@LDA (black solid line), G_0W_0@PBE (blue solid line), and G_0W_0@PBE0 (red solid region).

associated Cu *d*-CO HOMO/LUMO separation increases.

We note that the results shown in Figs. 3 and 4 are calculated for a finite cluster. In contrast to the adsorption energy, the DOS converges much slower with respect to cluster size, and the results in Figs. 3 and 4 will most likely change quantitatively in the infinite periodic limit. We expect, however, that the general trend PBE→PBE0→G_0W_0 is already captured in our finite cluster calculation. Comparing the three different G_0W_0 calculations (cf. Fig. 4), we again see a small starting-point dependence that is more pronounced for the CO than the Cu states. In accord with observations for bulk semiconductors,[62] the agreement for localized states with experiment is best when the self-interaction error is removed or reduced already in the ground-state calculation, as is the case for G_0W_0@ PBE0.

IV. CONCLUSION

In summary, the adsorption energies for CO on the Cu(111) surface have been calculated with the GGA functionals PBE and AM05, the hybrid functional PBE0 and HSE03, and in the RPA. PBE and AM05 predict the wrong hollow-site adsorption, in agreement with previous calculations,[27] whereas PBE0 and HSE03 yield a slight preference to the correct atop adsorption site. RPA improves over PBE0 and HSE03 by further stabilizing the atop adsorption by ~0.2 eV. The mechanism behind this improvement can be understood by analyzing the DOS calculated at the corresponding level of theory. We conclude that the adsorption energy calculated at the RPA level together with the associated G_0W_0 density of states offers a powerful approach for tackling the CO-adsorption puzzle and may be a valuable tool for other intricate adsorption problems where LDA and GGA calculations fail.

ACKNOWLEDGMENTS

We would like to acknowledge fruitful discussions with Karsten Reuter, Volker Blum, Hong Jiang, and Martin Fuchs. This work was in part funded by the EU's 6th framework program through the NANOQUANTA (Grant No. NMP4-CT-2004-500198) network of excellence.

*xinguo@fhi-berlin.mpg.de

[1] H. Steininger, S. Lehwald, and H. Ibach, Surf. Sci. **123**, 264 (1982).
[2] G. S. Blackman, M.-L. Xu, D. F. Ogletree, M. A. Van Hove, and G. A. Somorjai, Phys. Rev. Lett. **61**, 2352 (1988).
[3] J. Kessler and F. Thieme, Surf. Sci. **67**, 405 (1977).
[4] R. Raval, S. F. Parker, M. E. Pemble, P. Hollins, J. Pritchard, and M. A. Chesters, Surf. Sci. **203**, 353 (1988).
[5] P. J. Feibelman, B. Hammer, J. K. Nørskov, F. Wagner, M. Scheffler, R. Stumpf, R. Watwe, and J. Dumestic, J. Phys. Chem. B **105**, 4018 (2001).
[6] A. Gil, A. Clotet, J. M. Ricart, G. Kresse, M. García-Hernández, N. Rösch, and P. Sautet, Surf. Sci. **530**, 71 (2003).
[7] M. Gajdoš, A. Eichler, and J. Hafner, J. Phys.: Condens. Matter **16**, 1141 (2004).
[8] R. A. Olsen, P. H. T. Philipsen, and E. J. Baerends, J. Chem. Phys. **119**, 4522 (2003).
[9] Y. M. Niquet, M. Fuchs, and X. Gonze, Phys. Rev. A **68**, 032507 (2003).
[10] J. F. Dobson, A. White, and A. Rubio, Phys. Rev. Lett. **96**, 073201 (2006).
[11] N. E. Dahlen and U. von Barth, Phys. Rev. B **69**, 195102 (2004).
[12] H. Jiang and E. Engel, J. Chem. Phys. **127**, 184108 (2007).
[13] F. Furche, Phys. Rev. B **64**, 195120 (2001).
[14] M. Fuchs and X. Gonze, Phys. Rev. B **65**, 235109 (2002).
[15] J. F. Dobson and J. Wang, Phys. Rev. Lett. **82**, 2123 (1999).
[16] P. García-González, J. J. Fernández, A. Marini, and A. Rubio, J. Phys. Chem. A **111**, 12458 (2007).
[17] A. Marini, P. García-González, and A. Rubio, Phys. Rev. Lett. **96**, 136404 (2006).
[18] J. Harl and G. Kresse, Phys. Rev. B **77**, 045136 (2008).
[19] M. Rohlfing and T. Bredow, Phys. Rev. Lett. **101**, 266106 (2008).
[20] J. Toulouse, I. C. Gerber, G. Jansen, A. Savin, and J. G. Ángyán, Phys. Rev. Lett. **102**, 096404 (2009).
[21] D. Lu, Y. Li, D. Rocca, and G. Galli, Phys. Rev. Lett. **102**, 206411 (2009).
[22] G. Kresse, A. Gil, and P. Sautet, Phys. Rev. B **68**, 073401 (2003).
[23] S. E. Mason, I. Grinberg, and A. M. Rappe, Phys. Rev. B **69**, 161401(R) (2004).
[24] M. Gajdoš and J. Hafner, Surf. Sci. **590**, 117 (2005).
[25] K. Doll, Surf. Sci. **573**, 464 (2004).
[26] M. Neef and K. Doll, Surf. Sci. **600**, 1085 (2006).
[27] A. Stroppa, K. Termentzidis, J. Paier, G. Kresse, and J. Hafner, Phys. Rev. B **76**, 195440 (2007).
[28] A. Stroppa and G. Kresse, New J. Phys. **10**, 063020 (2008).
[29] Q.-M. Hu, K. Reuter, and M. Scheffler, Phys. Rev. Lett. **98**, 176103 (2007).
[30] S. Sharifzadeh, P. Huang, and E. Carter, J. Phys. Chem. C **112**, 4649 (2008).
[31] L. Hedin, Phys. Rev. **139**, A796 (1965).
[32] J. Y. Saillard and R. Hoffmann, J. Am. Chem. Soc. **106**, 2006 (1984).
[33] R. A. van Santen and M. Neurock, Catal. Rev. - Sci. Eng. **37**, 557 (1995).
[34] G. Blyholder, J. Phys. Chem. **68**, 578 (1964).
[35] A. D. Becke, J. Chem. Phys. **98**, 5648 (1993).
[36] J. P. Perdew, M. Ernzerhof, and K. Burke, J. Chem. Phys. **105**, 9982 (1996).
[37] J. P. Perdew, K. Burke, and M. Ernzerhof, Phys. Rev. Lett. **77**, 3865 (1996).
[38] J. Heyd, G. E. Scuseria, and M. Ernzerhof, J. Chem. Phys. **118**, 8207 (2003).
[39] T. Helgaker, J. Gauss, P. Jørgensen, and J. Olsen, J. Chem. Phys. **106**, 6430 (1997).
[40] J. D. Talman and W. F. Shadwick, Phys. Rev. A **14**, 36 (1976).
[41] S. Kümmel and L. Kronik, Rev. Mod. Phys. **80**, 3 (2008).

[42] P. Rinke, A. Qteish, J. Neugebauer, C. Freysoldt, and M. Scheffler, New J. Phys. **7**, 126 (2005).
[43] D. Bohm and D. Pines, Phys. Rev. **92**, 609 (1953).
[44] M. Gell-Mann and K. A. Brueckner, Phys. Rev. **106**, 364 (1957).
[45] D. C. Langreth and J. P. Perdew, Phys. Rev. B **15**, 2884 (1977).
[46] O. Gunnarsson and B. I. Lundqvist, Phys. Rev. B **13**, 4274 (1976).
[47] J. P. Perdew and K. Schmidt, in *Density Functional Theory and Its Application to Materials*, edited by V. Van Doren, C. Van Alsenoy, and P. Geerlings (AIP, Melville, NY, 2001).
[48] W. Nelson, P. Bokes, P. Rinke, and R. W. Godby, Phys. Rev. A **75**, 032505 (2007).
[49] M. Hellgren and U. von Barth, Phys. Rev. B **76**, 075107 (2007).
[50] K. S. Singwi, M. P. Tosi, R. H. Land, and A. Sjölander, Phys. Rev. **176**, 589 (1968).
[51] F. Furche and T. Van Voorhis, J. Chem. Phys. **122**, 164106 (2005).
[52] F. Furche, J. Chem. Phys. **129**, 114105 (2008).
[53] M. E. Casida, Phys. Rev. A **51**, 2005 (1995).
[54] T. Kotani, J. Phys.: Condens. Matter **10**, 9241 (1998).
[55] Y. M. Niquet, M. Fuchs, and X. Gonze, J. Chem. Phys. **118**, 9504 (2003).
[56] U. von Barth, N. E. Dahlen, R. van Leeuwen, and G. Stefanucci, Phys. Rev. B **72**, 235109 (2005).
[57] M. Grüning, A. Marini, and A. Rubio, J. Chem. Phys. **124**, 154108 (2006).
[58] L. J. Sham and M. Schlüter, Phys. Rev. Lett. **51**, 1888 (1983).
[59] L. J. Sham and M. Schlüter, Phys. Rev. B **32**, 3883 (1985).
[60] R. W. Godby, M. Schlüter, and L. J. Sham, Phys. Rev. B **37**, 10159 (1988).
[61] W. G. Aulbur, L. Jönsson, and J. W. Wilkins, Solid State Phys., Adv. Res. Appl. **54**, 1 (2000).
[62] P. Rinke, A. Qteish, J. Neugebauer, and M. Scheffler, Phys. Status Solidi B **245**, 929 (2008).
[63] M. Grüning, A. Marini, and A. Rubio, Phys. Rev. B **74**, 161103(R) (2006).
[64] O. V. Gritsenko, P. R. T. Schipper, and E. J. Baerends, J. Chem. Phys. **107**, 5007 (1997).
[65] C. Freysoldt, P. Eggert, P. Rinke, A. Schindlmayr, and M. Scheffler, Phys. Rev. B **77**, 235428 (2008).
[66] V. Blum, F. Hanke, R. Gehrke, P. Havu, V. Havu, X. Ren, K. Reuter, and M. Scheffler, Comput. Phys. Comm. (to be published).
[67] X. Ren, A. Sanfilippo, V. Blum, P. Rinke, K. Reuter, and M. Scheffler (unpublished).
[68] K. P. Huber and G. Herzberg, *Constants of Diatomic Molecules* (Van Nostrand Reinhold, New York, 1979).
[69] R. D. Rempt, Phys. Rev. Lett. **22**, 1034 (1969).
[70] R. Armiento and A. E. Mattsson, Phys. Rev. B **72**, 085108 (2005).
[71] S. Vollmer, G. Witte, and C. Woell, Catal. Lett. **77**, 97 (2001).
[72] P. A. Redhead, Vacuum **12**, 203 (1962).
[73] B. E. Hayden, K. Kretzschmar, and A. M. Bradshaw, Surf. Sci. **155**, 553 (1985).